CHAPTER 57

Fully Nonlinear Properties of Periodic Waves Shoaling over Slopes

Stéphan T. Grilli¹, M. ASCE, and Juan Horrillo²

ABSTRACT : Shoaling of finite amplitude periodic waves over a sloping bottom is calculated in a *numerical wave tank* which combines : (i) a Boundary Element Model to solve Fully Nonlinear Potential Flow (FNPF) equations; (ii) an exact generation of *zero-mass-flux Streamfunction Waves* at the deeper water extremity; and (iii) an *Absorbing Beach* (AB) at the far end of the tank, which features both free surface absorption (through applying an external pressure) and lateral active absorption (using a piston-like condition). A feedback mechanism adaptively calibrates the beach absorption coefficient, as a function of time, to absorb the period-averaged energy of incident waves.

Shoaling of periodic waves of various heights and periods is modeled over 1:35, 1:50, and 1:70 slopes (both plane and natural), up to very close to the breaking point. Due to the low reflection from both the slope and the AB, a quasi-steady state is soon reached in the tank for which local and integral properties of shoaling waves are calculated $(K_s, c, H/h, kH, \eta_m, S_{xx},...)$. Comparisons are made with classical wave theories and observed differences are discussed. Parameters providing an almost one-to-one relationship with relative depth kh in the shoaling region are identified. These could be used to solve the so-called *depth-inversion problem*.

INTRODUCTION

In the coastal region, incident ocean waves propagating towards the shore (in direction x; Fig. 1) increasingly feel the effects of the reducing depth h(x), due to the sloping ocean bottom. These effects induce significant changes in wave shape, height H, length L, and phase celerity c, while the wave period T stays closely constant. Predicting such changes (usually referred to as *wave shoaling*) up to the point waves become unstable and break (breaking point; BP) is one of the important tasks of coastal

¹Distinguished Assoc. Professor, Dept. of Ocean Engng., University of Rhode Island, Narragansett-RI 02882, USA, email: grilli@oce.uri.edu, http://www.oce.uri.edu/~grilli

²Graduate Student, same address

engineering. Characteristics of waves at the BP indeed are used to design coastal structures and predict littoral sediment transport; detailed wave kinematics at the BP is also needed for surfzone models which are increasingly used in coastal engineering research and design. In the more specific problem referred to as *depth inversion*, one seeks to predict the nearshore bottom topography based on observed characteristics of shoaling waves (e.g., through remote sensing). Hence, simple relationships between these and h(x) are sought after.

In most wave transformation models used so far, shoaling of deep water waves is calculated based on linear or weakly nonlinear theories (e.g., modified Boussinesq eqs.) and using semi-empirical breaking criteria to locate the BP. Such theories, however, despite their satisfactory predictions in deep and intermediate water, may not be sufficiently accurate close to the BP where wave height reaches a significant fraction of the depth. Highly nonlinear waves have been modeled using a higher-order Fourier steady-wave theory (FSWT), e.g., by Sobey and Bando³ (1991). In the latter work, up to three conservation equations for mass, momentum, and energy flux, are expressed to propagate incident waves over a mildly sloping bottom. In such an approach, however, the bottom slope is replaced by a cascade of horizontal steps and, hence, wave profiles do not take the characteristic skewed shape observed in experiments before breaking occurs. As a result, wave kinematics and dynamics cannot be well represented close to the BP⁴. Finally, in this approach, breaking corresponds to the highest wave which is stable over constant depth. This is quite unrealistic since, as we will see, skewness and unsteadiness allow waves to reach a larger height before they break.

To accurately predict wave properties close to the BP, we will show that, in addition to full nonlinearity, even for mild slopes, the influence of bottom topography on wave shape must be included in shoaling models. Time dependent models based on fully nonlinear potential flow (FNPF) theory have this capability, provided proper wave generation and absorption methods are implemented (e.g., 2D : Klopman, 1988; Grilli *et al.*, 1989; Cointe, 1990, Cooker, 1990; Ohyama and Nadaoka, 1991; 3D : Romate, 1989; Broeze, 1993). Hence, with such models, a "numerically exact" solution can be obtained for waves shoaling over an arbitrary bottom geometry, for which no approximation other than potential flow theory is made.

NUMERICAL MODEL

The two-dimensional FNPF model by Grilli, *et al.* (1989, 1990, 1996) will be used to compute characteristics of periodic waves shoaling over both plane and natural slopes, up to a very high fraction of the breaking height (Fig. 1). FNPF computations can

³Also see their detailed review of other similar works. Note, Johnson and Arneborg (1995) followed a similar approach using a fourth-order perturbation method.

⁴The authors nevertheless assume that integral properties should be insensitive to such details and are thus well predicted by a FSWT. The latter assumption is quite questionable, since radiation stresses, for instance, are strongly influenced by wave skewness.

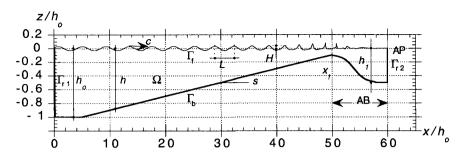


Figure 1: Sketch for FNPF computations of a periodic wave shoaling over a plane slope s, in a "numerical wave tank".

model overturning waves but, by nature, are limited to prior to the time touch-down of a breaker jet first occurs. This does not pose problems when solitary waves are used in the analysis, as it has often been the case in the past ⁵. For periodic or irregular waves, however, an *absorbing beach* (AB) must be used to absorb the energy of incident waves, hence eliminating reflection and preventing these from breaking at the top of the slope.

Grilli and Horrillo (1996) implemented such an AB in the model over a shallower region located in the upper part of the slope whose geometry was specified somewhat similar to natural bars on beaches⁶ (Fig. 1). Energy absorption combined both free surface and lateral absorption with an adaptive calibration of the absorption coefficient : (i) an exterior counteracting pressure is specified on the AB free surface, proportional to the normal particle velocity (Cointe, 1990; Cao et al., 1993), to create a negative work against incident waves; this is shown to absorb high frequency wave energy well; (ii) a piston-like (active) absorbing boundary condition is specified at the tank extremity Γ_{r2} ("absorbing piston", AP), which is shown to absorb low frequency wave energy well (Clément, 1996); (iii) the AB's absorption coefficient is adaptively calibrated in time to absorb the period-averaged energy of incident waves entering the beach at $x = x_i$. Grilli and Horrillo developed and tested this AB and showed that wave reflection could be reduced to a few percent only. Hence, in a "numerical wave tank" such as sketched in Fig. 1, computations for periodic waves can reach a quasi-steady state for which properties of shoaling waves can be calculated, up to very close to the BP, and compared to results of other shoaling methods (theory or models), which usually assume there is no reflection from the slope or beach. [In the present method, reflection from the slope still occurs as it does in nature.]

Incident waves can be arbitrary in the model but, for sake of comparison with other wave theories, permanent form wave solutions of the FNPF problem are generated on the leftward boundary (Γ_{r1} , Fig. 1). These are so-called streamfunction waves

⁵In such cases, FNPF calculations can predict characteristics of breaking solitary waves within 2% of experimental measurements (Grilli *et al.*, 1994, 1997)

⁶In this case, gradual deshoaling of waves occurs in the AB which helps absorbing wave energy.

(SFW; Dalrymple 1974; Dean and Dalrymple 1984) which, unlike finite amplitude waves produced by a wavemaker, do not exhibit the generation of higher harmonics and the beat phenomenon observed in wave tanks as they propagate over constant depth (e.g., Chapalain *et al.*, 1996). Since SFW's have a non-zero mass flux, they are generated in the model together with a mean current, equal and opposite to their period-averaged mass transport velocity (Grilli and Horrillo, 1996). Hence, volume stays constant within the "numerical wave tank" as it would on a beach for which the undertow current balances the incident mass flux at some distance from the shore.

Details of model equations, numerical methods and validation applications can be found in the above-referenced papers. It will just be mentioned that Laplace's equation is solved in the model, over domain Ω , based on a higher-order Boundary Element Method (BEM) derived from Green's 2nd identity. Boundaries are discretized using N nodes and M higher-order elements are specified to interpolate in between the nodes. Quadratic isoparametric elements are used on lateral and bottom boundaries $(\Gamma_{r1}, \Gamma_{r2}, \Gamma_b)$ and cubic elements ensuring continuity of the slope are used on the free surface boundary Γ_f (Grilli and Subramanya 1996). The nonlinear free surface kinematic and dynamic boundary conditions are time integrated using second-order Taylor series expansions expressed in terms of a time step Δt and of the Lagrangian time derivative. Numerical errors are kept to a very small value by adaptively selecting the time step based on a mesh Courant number $C_{o}(t)$ (Grilli and Svendsen, 1990; Grilli and Subramanya 1996). In shoaling computations, as waves become increasingly steep towards the top of the slope, discretization nodes may get quite close to each other and create quasi-singular values for the BEM integrals, leading to poor accuracy. Hence, the adaptive regridding method developed by Grilli and Subramanya (1996) is used to automatically regrid nodes three by three when the distance between two nodes is either more than 4 times or less than 0.25 times the distance between the previous two nodes. In the following applications, a minimum of 20 nodes per wavelength is maintained throughout shoaling.

APPLICATIONS

Figure 1 illustrates a typical set-up for shoaling computations : (i) incident zeromass-flux SFW's are generated on Γ_{r1} (in depth h_o , with height H_o and period T; o-indices denote deep water values); (ii) waves propagate up the sloping bottom and are absorbed in the AB/AP; (iii) since reflection is very small from both the sloping bottom and the beach, computations soon reach a quasi-steady state for which successive waves undertake similar transformations (see Grilli and Horrillo, 1996, for a detailed discussion of numerical parameters and results); (iv) model parameters are tuned-up to let incident waves shoal up to impending overturning before they are absorbed in the AB. Numerical "wave gages" are specified at several fixed locations, $x = x_g$, over the slope where wave characteristics are calculated, both on the free surface (e.g., elevation $\eta(x_g, t)$) and as a function of depth z (e.g., velocity $\mathbf{u}(x_g, z, t)$, dynamic pressure $p_D(x_g, z, t)$).

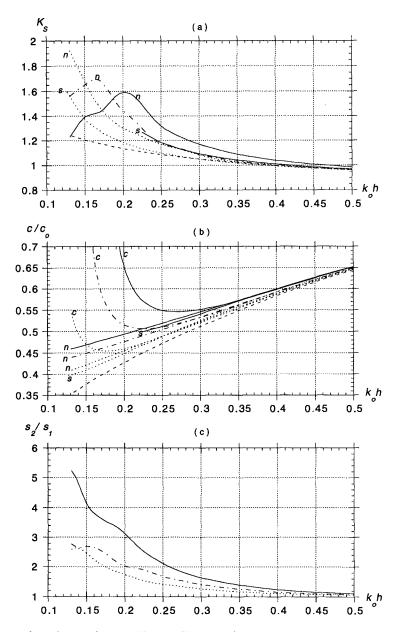


Figure 2: (a) shoaling coefficient $K_s = H/H_o$; (b) celerity c; and (c) left/right asymmetry s_2/s_1 , for periodic waves shoaling over a 1:50 slope, with $H'_o = H_o/h_o =$ (---) 0.04, (---) 0.06, and (---) 0.08, and $T' = T\sqrt{g/h_o} = 5.5$: (n) FNPF results; (s) Sobey and Bando's (1991) FSWT results; (--) LWT results; (c) CWT results. $c_o = gT/(2\pi)$ is the (linear) deep water celerity.

Local wave properties

After quasi-steady state is reached, successive incident waves are identified and tracked in the results : (i) envelopes of crest and trough elevations are calculated, from which wave height H(x) and shoaling coefficient $K_s(x) = H/H_o$ are obtained; (ii) phase velocity c(x) is calculated from the time derivative of crest trajectories; (iii) to quantify wave skewness, forward and backward normalized wave slopes are calculated as, $s_2(x) = H_2/(s_o L_2)$ and, $s_1(x) = H_1/(s_o L_1)$, respectively, in which (L_1, L_2) and (H_1, H_2) denote horizontal and vertical distances from a crest to the previous and next troughs, respectively, and $s_o = 2H_o/L_o = k_o H_o/\pi$. Results show that these quantities are quite well reproduced as a function of x, for successive incident waves (Grilli and Horrillo, 1996); in the applications, however, to eliminate small variations, ensemble averages of these quantities for each x are calculated over at least 4 successive waves.

In the model, waves are found to shoal up the slope, qualitatively, as expected from linear wave theory (Fig. 1): (i) both wavelength L and celerity c = L/Tcontinuously decrease; (ii) deshoaling first occurs, with a reduction in wave height, followed by shoaling and an increase in wave height up to the top of the slope where waves almost reach overturning before entering the AB and decaying.

More specifically, in Fig. 2, K_s , c, and s_2/s_1 have been plotted as a function of normalized depth $k_o h$, for a bottom slope s = 1:50 and three incident waves of normalized incident height $H'_{o} = H_{o}/h_{o} = 0.04, 0.06$, and 0.08, and normalized period $T' = T \sqrt{g/h_o} = 5.5 \ (k_o = (2\pi)^2/(gT^2)$ is the (linear) deep water wavenumber). Results of linear (LWT) and cubic (CWT) Stokes wave theories are also indicated. For $k_o h < 0.5$, significant differences are observed between FNPF results and the wave theories; this also corresponds to $kh = 2\pi h/L < 0.77$ (or H/h > 0.10; see Fig. 4b). For diminishing depths, due to increased nonlinearity, both K_{s} and c become significantly larger than predicted by LWT (Figs. 2a and 2b) and, as could be expected, increasingly so with the incident wave height. CWT predicts celerity better for shallower depths but diverges in very shallow water. The more accurate FSWT performs reasonably well for predicting celerities (Fig. 2b) but does quite poorly for wave heights (Fig. 2a). This is likely due to the lack of skewness in modeled waves whereas FNPF results for s_2/s_1 (Fig. 2c) show that waves are significantly skewed—i.e., forward tilted, left/right asymmetric—for very shallow water (see also Fig. 1 for spatial wave profiles).

The significant differences observed in Fig. 2 between FSWT and FNPF results show that, even for a very mild slope, the influence of actual bottom shape on local wave properties is important. Fig. 3 now investigates how this influence varies with bottom slope. An incident wave with $H'_o = 0.06$ and T' = 5.5 is shoaled up three plane beaches of slopes s = 1:35, 1:50, and 1:70, and a "natural beach" geometry with an average slope of 1:50. The natural beach has a depth variation defined according to Dean's equilibrium beach profile, $h = A(x^* - x)^{2/3}$, with x^* denoting a constant, function of the location of the toe of the slope in depth h_o , and A depending on the

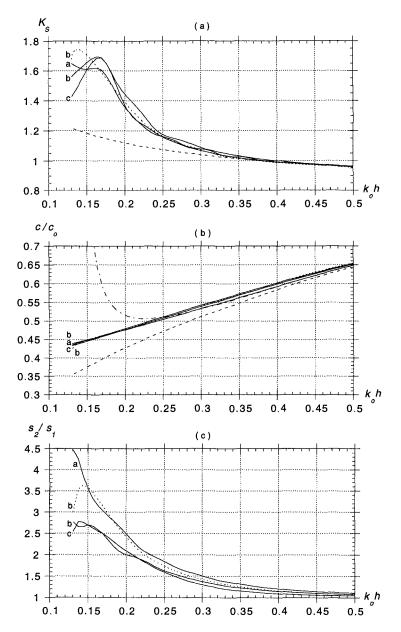


Figure 3: FNPF results for : (a) shoaling coefficient; (b) celerity; and (c) left/right asymmetry, for periodic waves with $H'_o = 0.06$ and T' = 5.5, on : 1:35 (curve a); 1:50 (curve b); 1:70 (curve c), plane (----) or natural (----) beaches. (---) LWT results; (----) CWT results.

specified average slope. This "natural beach", hence, has a milder slope in deeper water and a steeper slope in shallower water. For the wave height and celerity, Figs. 3a and 3b show fairly small differences between results calculated for the same depth on various slopes, for most of the shoaling region. The wave left/right asymmetry— s_2/s_1 , shown in Fig. 3c—seems to be more sensitive to bottom slope, becoming larger for the shallower parts of the (steeper) 1:35 slope and the "natural beach". Overall, however, no major differences are observed provided wave properties are compared for the same normalized depth.

Results in Fig. 3 imply that, for a given depth, local wave properties vary little for the same wave propagating over a range of mild slopes from 1:35 to 1:70. Hence, a broader parametric study will be carried out on a 1:50 slopes only, for 9 waves combining heights, $H'_{o} = 0.04$, 0.06, and 0.08 and period, T' = 5.5, 6.5, and 7.5. Results for each wave are given in Fig. 4 as a function, this time (due to the varying wave period), of the relative local depth kh. First, in Fig. 4a, we see that, for the phase celerity normalized by the linear wave celerity, $c_l = c_o \tanh kh$, the larger the incident wave height and the smaller the period (or similarly the larger $k_o H_o$) then, for a given kh, the larger the celerity increase with respect to q. Such results illustrate the well known amplitude dispersion effects due to increasing wave steepness ^{7}kH which, for the studied cases in shallow water $(kh < \pi/10)$, lead to a 40 to 85% maximum increase in celerity with respect to linear wave theory. In Fig. 4b, we see that, in all cases, the wave height to depth ratios H/h reach $\mathcal{O}(1)$ values in the shallow water region, confirming the very strong nonlinearities. A similar analysis of shoaling coefficients would show that linear wave theory significantly underpredicts wave height for depths corresponding to H/h > 0.2 (which also corresponds to the region where celerity is significantly underpredicted in Fig. 4a); for the studied cases this underprediction of K_{\bullet} is up to 55%. With regard to these results, it is anticipated that the quantity, $kH/(k_oH_o) = K_s/(c/c_o)$, i.e., the local wave steepness normalized by the deep water steepness, should exhibit somewhat less variations (i.e., overprediction) with respect to linear wave results, since underprediction of wave height and celerity should compensate each other to some extent. This is confirmed in Fig. 4c where we see, first of all, that all FNPF results follow quite a similar increase as a function of kh, up to maximum steepness, and that results of LWT (i.e., K_s / tanh kh) are a better predictor of normalized wave steepness, with a maximum underprediction of only 11%, than for the other wave properties discussed above. Considering the many differences in wave shape, height and length, and kinematics, observed between FNPF and LWT results, the latter result is somewhat unexpected.

Integral wave properties

These are the mean water level η_m , the mean undertow current U_m , the energy flux E_f , and the radiation stress S_{xx} . In the model, integral properties are computed at

⁷Such effects are predicted at third-order by Stokes theory (CWT).

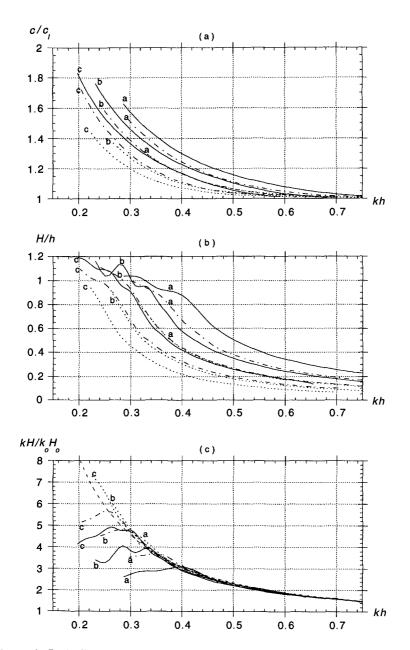


Figure 4: Periodic waves shoaling over a 1:50 slope. $H'_o = (---) 0.04, (----) 0.06$, and (----) 0.08, and T' = : 5.5 (curves a); 6.5 (curves b); 7.5 (curves c). (----) LWT results; $c_l = c_o \tanh kh$, is the linear wave celerity.

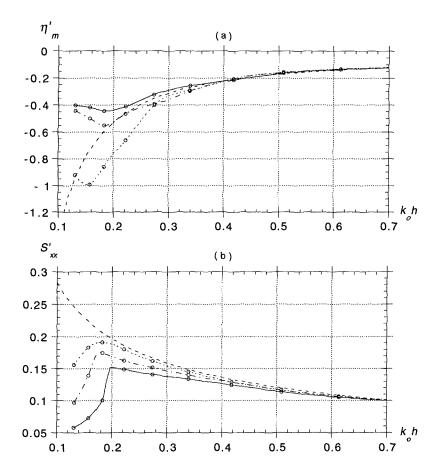


Figure 5: Normalized (a) mean water level $\eta'_m = \eta_m / h_o H_o'^2$; and (b) radiation stress $S'_{xx} = S_{xx} / \rho g H_o^2$ (with ρ the fluid density), for three periodic waves shoaling over a 1:50 slope. Symbols and definitions are as in Fig. 2. Results have been averaged over 3T in the quasi-steady regime. Symbols (\circ) denote locations $x = x_g$ of "numerical gages". Corrections, $\Delta \eta'_{mo} = -0.0274$ and $\Delta S'_{xxo} = h'_o (\Delta \eta'_{mo}) + (\Delta \eta'_{mo})^2/2$, have been applied to the linear results for η'_m and S'_{xx} , respectively, to account for the actual mean water level in depth h_o in the FNPF results.

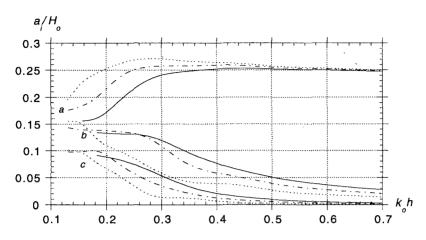


Figure 6: Normalized amplitudes of first three harmonics (a,b,c), a_i (i = 1,2,3), for three periodic waves shoaling over a 1:50 slope. Definitions are as in Fig. 2.

"numerical gages" located at $x = x_g$ above the sloping bottom using classical equations, i.e., through depth integrations and wave period-averaging involving, $\eta(x_g, t)$, $u(x_g, z, t)$ and $p_D(x_g, z, t)$. To account for the non-zero mean Eulerian velocity in the model (resulting from specifying zero-mass-flux incident waves at boundary Γ_{r1}), and for the set-down η_m , expressions of integral properties are corrected following Klopman (1990) and Jonsson and Arneborg (1995). In the model, time averaging is performed at time t, for the results calculated from time t - T to t. Time series of integral properties are thus obtained for each gage location x_g . When computations reach a quasi-steady state, integral properties stabilize to fairly constant values in time for each gage location. To eliminate small time fluctuations and oscillations of integral properties with respect to these constant values, averages are calculated over 3T, before results are analyzed.

In all cases, the energy flux is found to be very close to constant at the gages located in the region where wave height increases (e.g., over the shoaling parts of curves in Figs. 2a and 3a). This indicates that reflection is small from both the sloping bottom and from the AB. As depth decreases, the mean undertow current increases roughly proportionally to 1/h, as expected from the period-averaged continuity equation, and then decreases when wave height starts decreasing.

Mean water level and radiation stress results are given in Fig. 5, for the same three waves as in Fig. 2, shoaling over a 1:50 slope. As expected, the normalized η_m in Fig. 5a follows a trend opposite to S_{xx} in Fig. 5b, first setting-down over the slope and then stabilizing towards the top of the slope and increasing in the AB due to wave height reduction. In shallow water, the set-down becomes relatively larger, the smaller the incident wave, as a result of the steeper drop in radiation stresses for the larger waves. Results obtained from a first-order nonlinear perturbation of LWT (FNLT; Dean and Dalrymple, 1984) and adjusted to match the initial FNPF set-down in depth h_o , show reasonable agreement with FNPF results. In the shallower region at the top of the slope, however, FNLT results do not capture the leveling-up of η_m . Radiation stresses in Fig. 5b gradually increase while wave height increases and depth decreases, following the expected pattern from FNLT, which predicts results quite well in the deeper water region. At some stage, however, FNPF results become smaller than FNLT results, and more so, for a given depth, the larger the incident wave height. A more detailed analysis of these results would show that this decrease in S_{xx} is strongly correlated with the increase in "skewness index" s_2/s_1 , shown earlier in Fig. 2c for $k_o h < 0.45$; this confirms that radiation stresses are quite sensitive to wave shape.

Fourier analysis

Another way of analyzing how wave shape changes during shoaling is to calculate Fourier transforms of wave surface elevations $\eta(x_g, t)$ obtained at fixed gages at $x = x_g$. Harmonic amplitudes can then be plotted as a function of x_g . This was done in Fig. 6 which shows normalized amplitudes of the first three harmonics a_i (i = 1,2,3), for the same three waves as in Fig. 2 shoaling over a 1:50 slope. In all cases, in the shoaling region where wave height increases (Fig. 2a), after a slight initial increase, a_1 decreases while a_2 and a_3 continuously increase. This indicates that, in shoaling periodic waves, energy is being continuously transferred to higherorder harmonics, as a result of nonlinear interactions. As could be expected, for a given depth, this nonlinear energy exchange is stronger, the larger the incident wave height, and the energy transfer to the higher-order harmonics thus starts occurring in deeper water. Not surprisingly, variations of the "skewness index" s_2/s_1 in Fig. 2c are strongly correlated with variations of a_2 and (particularly) of a_3 in Fig. 6.

Conclusions

A numerical wave tank was used to model finite amplitude periodic waves shoaling over a sloping bottom. Periodic waves of various heights and periods, covering the range $k_o H_o = [0.028, 0.105]$, were modeled over 1:35, 1:50, and 1:70 slopes (both plane and natural), up to very close to the breaking point. Due to the low reflection from the slope and the AB, a quasi-steady state was soon reached in the tank for which both local and integral properties of fully nonlinear shoaling waves were calculated $(K_s, c, s_2/s_1 (left/right asymmetry), H/h, kH, \eta_m, S_{xx})$.

For a shallow enough normalized depth ($k_o h < 0.5$ or kh < 0.77), significant differences are observed between FNPF results and 1st (LWT), 3rd (CWT), and higherorder steady wave (FSWT) theories. For the first two theories, low-order nonlinearity is clearly the main reason for the observed differences in a region where H/h = O(1); in the latter theory, the lack of wave skewness and the representation of the bottom by horizontal steps likely explain the observed differences. Despite the significant effects of actual bottom shape on the results, for the range of tested mild slopes, FNPF results are found fairly similar for the same wave taken at the same normalized depth $(k_oh \text{ or } kh)$. This, hence, allows us to use kh as the *unique parameter* describing a mild bottom variation and to compute additional results on a unique mild slope (1:50). In these results, for the range of tested waves, the normalized wave steepness, kH/k_oH_o , shows an almost one-to-one relationship with kh in the shoaling region. Steepness thus could be used to solve the so-called *depth-inversion problem*. Quite surprisingly, due to a partial compensation of nonlinear effects for the wave height and celerity, LWT is found quite a good predictor of this parameter (maximum difference is 11%), whereas discrepancies for H and c reach 55 and 85%, respectively.

For the tested waves, set-down is quite well predicted by the first-order perturbation of LWT, except in the shallower region, where it is smaller, following the steep drop in radiation stresses. [This could also be partly due to the mean undertow current. More work remains to be done about this.]. Radiation stresses are overpredicted by the first-order theory in the region where wave left/right asymmetry s_2/s_1 (i.e., skewness) becomes large, confirming the sensitivity of this parameter to wave shape. Otherwise, agreement with the theory is quite good. A Fourier analysis of surface profiles $\eta(x_g, t)$ calculated for gages located at $x = x_g$ shows a continuous transfer of energy from the fundamental to higher-order harmonics in the shoaling region, illustrating nonlinear interactions in the shoaling wave field. The 3rd-harmonic amplitude a_3 is strongly correlated with s_2/s_1 .

Acknowledgments

This publication is the result of research sponsored by the US Naval Research Laboratory, Stennis Space Center, grants N-00014-95-1-G607 and N-00014-96-C012, from the Remote Sensing Division (code 7240). The kind assistance of Dr. Peter Smith is gratefully acknowledged.

References

- [1] Broeze, J., Numerical Modelling of Nonlinear Free Surface Waves With a 3D Panel Method. Ph.D. Dissertation, Enschede, The Netherland, 1993.
- [2] Cao, Y., Beck, R.F. and Schultz, W.W., An Absorbing Beach for Numerical Simulations of Nonlinear Waves in a Wave Tank. *Proc. 8th Intl. Workshop Water Waves and Floating Bodies* (St. John's, 5/93) pps. 17-20, 1993.
- [3] Chapalain, G., Cointe, R. and Temperville, A., Observed and Modeled Resonantly Interacting Progressive Water-waves. *Coastal Engng.*, 16, 267-300, 1996.
- [4] Clément, A., Coupling of Two Absorbing Boundary Conditions for 2D Timedomain Simulations of Free Surface Gravity Waves. J. Comp. Phys., 126, 139-151, 1996.

- [5] Cointe, R., Numerical Simulation of a Wave Channel. Engng. Analysis with Boundary Elements, 7 (4), 167-177, 1990.
- [6] Cooker, M.J., A Boundary-integral Method for Water Wave Motion over Irregular Bed. Engng. Analysis with Boundary Elements, 7 (4), 205-213, 1990.
- [7] Dalrymple, R.A., 1974, A Finite Amplitude Wave on a Linear Shear Current, J. Geophys. Res., 79(30), 4498-4504.
- [8] Dean, R.G. and Dalrymple R.A., Water Wave Mechanics for Engineers and Scientists Prentice-Hall, 1984.
- [9] Grilli, S.T., and J., Horrillo, Numerical Generation and Absorption of Fully Nonlinear Periodic Waves. J. Engng. Mech. (accepted), 1996.
- [10] Grilli, S., Skourup, J., and Svendsen, I.A., An Efficient Boundary Element Method for Nonlinear Water Waves, Engng. Analysis with Boundary Elements, 6(2), 97-107, 1989.
- [11] Grilli, S.T. and Subramanya, R., Numerical Modeling of Wave Breaking Induced by Fixed or Moving Boundaries. *Computational Mech.*, **17**, 374-391, 1996.
- [12] Grilli, S.T., Subramanya, R., Svendsen, I.A. and Veeramony, J., Shoaling of Solitary Waves on Plane Beaches. J. Waterway Port Coastal and Ocean Engng., 120 (6), 609-628, 1994.
- [13] Grilli, S. and Svendsen, I.A., Corner Problems and Global Accuracy in the Boundary Element Solution of Nonlinear Wave Flows, *Engng. Analysis with Boundary Elements*, 7(4), 178-195, 1990.
- [14] Grilli, S.T., Svendsen, I.A. and Subramanya, R., Breaking Criterion and Characteristics for Solitary Waves on Plane Beaches. J. Waterway Port Coastal and Ocean Engng., 123 (3) (in press), 1997.
- [15] Jonsson, I.G. and Arneborg, L., Energy Properties and Shoaling of Higher-order Stokes Waves on a Current. Ocean Engng., 22 (8), 819-857, 1995.
- [16] Klopman, G., Numerical Simulation of Gravity Wave Motion on Steep slopes. Delft Hydraulics Report No. H195, 1988.
- [17] Klopman, G., A Note on Integral Properties of Periodic Gravity Waves in the Case of a Non-zero Mean Eulerian Velocity. J. Fluid Mech. 211, 609-615, 1990.
- [18] Ohyama, T. and Nadaoka, K., Development of a Numerical Wave Tank for Analysis of Nonlinear and Irregular Wave Fields. *Fluid Dyn. Res.* 8, 231-251, 1991.
- [19] Romate, J.E., The Numerical Simulation of Nonlinear Gravity Waves in Three Dimensions using a Higher Order Panel Method. *Ph.D. Dissertation. Department of Applied Mathematics, University of Twente, The Netherland,* 1989.